

Strongly enhanced vortex pinning from 4 to 77 K in magnetic fields up to 31 T in 15 mol.% Zr-added (Gd, Y)-Ba-Cu-O superconducting tapes

Cite as: APL Mater. 2, 046111 (2014); <https://doi.org/10.1063/1.4872060>

Submitted: 14 February 2014 • Accepted: 10 April 2014 • Published Online: 23 April 2014

A. Xu, L. Delgado, N. Khatri, et al.



View Online



Export Citation



CrossMark

ARTICLES YOU MAY BE INTERESTED IN

[High critical currents in heavily doped \(Gd,Y\)Ba₂Cu₃O_x superconductor tapes](#)

Applied Physics Letters **106**, 032601 (2015); <https://doi.org/10.1063/1.4906205>

[Broad temperature range study of J_c and H_{irr} anisotropy in YBa₂Cu₃O_x thin films containing either Y₂O₃ nanoparticles or stacking faults](#)

Applied Physics Letters **106**, 052603 (2015); <https://doi.org/10.1063/1.4907891>

[Improvement in J_c performance below liquid nitrogen temperature for SmBa₂Cu₃O_y superconducting films with BaHfO₃ nano-rods controlled by low-temperature growth](#)

APL Materials **4**, 016102 (2016); <https://doi.org/10.1063/1.4939182>



THE ADVANCED MATERIALS MANUFACTURER®

yttrium iron garnet	glassy carbon	beam splitters	fused quartz	additive manufacturing
zeolites	UV-V visible reducers	calcium halides	taper nanoparticles	organic materials
nano ribbons	barium fluoride	europium phosphors	piezotronics	infrared dyes
optical crystal growth	ultra high purity mesocells	transparent ceramics	COG	
synthetics	nan-YAG	resin oxide polishing powders	semiconductors	thin films
silver nanoparticles	perovskites	surface functionalized nanoparticles	WBG grade materials	thin films
MOCVD	beta barium borate		OLED lighting	semiconductors
rare earth metals	quantum dots		sputtering targets	fiber optics
cerium	solid solution Gd ₂ O ₃		In-Sn	deposition slugs
refractory metals	laser crystals		CVD precursors	photoconductive
anode	lithium nitrate	InAs wafers	metamaterials	laser case glass
deposition oxides	MOPs	AlN	YBCO	superconductors
chalcogenides	ZnS	CdTe	indium tin oxide	MgO
barium titanate crystals	transparent ceramics		diamond microcutter	optical glass

The Next Generation of Material Science Catalogs



Strongly enhanced vortex pinning from 4 to 77 K in magnetic fields up to 31 T in 15 mol.% Zr-added (Gd, Y)-Ba-Cu-O superconducting tapes

A. Xu,^{1,a} L. Delgado,¹ N. Khatri,¹ Y. Liu,¹ V. Selvamanickam,¹ D. Abraimov,² J. Jaroszynski,² F. Kametani,² and D. C. Larbalestier²

¹Department of Mechanical Engineering and Texas Center for Superconductivity, University of Houston, Houston, Texas 77204, USA

²Applied Superconductivity Center, National High Magnet Field Laboratory, Florida State University, Tallahassee, Florida 32310, USA

(Received 14 February 2014; accepted 10 April 2014; published online 23 April 2014)

Applications of REBCO coated conductors are now being developed for a very wide range of temperatures and magnetic fields and it is not yet clear whether vortex pinning strategies aimed for high temperature, low field operation are equally valid at lower temperatures and higher fields. A detailed characterization of the superconducting properties of a 15 mol. % Zr-added REBCO thin film made by metal organic chemical vapor deposition, from 4.2 to 77 K under magnetic fields up to 31 T is presented in this article. Even at a such high level of Zr addition, T_c depression has been avoided ($T_c = 91$ K), while at the same time an exceptionally high irreversibility field $H_{irr} \approx 14.8$ T at 77 K and a remarkably high vortex pinning force density $F_p \approx 1.7$ TN/m³ at 4.2 K have been achieved. We ascribe the excellent pinning performance at high temperatures to the high density (equivalent vortex matching field ~ 7 T) of self-assembled BZO nanorods, while the low temperature pinning force is enhanced by large additional pinning which we ascribe to strain-induced point defects induced in the REBCO matrix by the BZO nanorods. Our results suggest even more room for further performance enhancement of commercial REBCO coated conductors and point the way to REBCO coil applications at liquid nitrogen temperatures since the critical current density $J_c(H//c)$ characteristic at 77 K are now almost identical to those of fully optimized Nb-Ti at 4 K. © 2014 Author(s). All article content, except where otherwise noted, is licensed under a Creative Commons Attribution 3.0 Unported License. [<http://dx.doi.org/10.1063/1.4872060>]

Thanks to its high critical temperature T_c , high critical current density J_c , high irreversibility field H_{irr} , and moderate anisotropy parameter γ , REBa₂Cu₃O_x (REBCO, where RE = rare earth) thin films grown on flexible and mechanically strong substrates can exceed the temperature and field application limits of the Nb-based low temperature superconductors, and enable superconducting applications in a broad temperature and magnetic field regime now exceeding 35 T at 4 K.¹⁻³ However, further J_c and H_{irr} enhancement and anisotropy reduction are strongly desirable for compelling, cost-effective applications, and especially to enable multi-Tesla fields in a temperature regime of 30–77 K.⁴⁻⁶ Enhanced vortex pinning is needed both to raise higher temperature irreversibility fields and to raise J_c so that overall conductor current density J_E can reach the required high values of the order of 500 A/mm². Adding higher densities of nanoscale defects with strong vortex pinning properties is the most efficient strategy.^{7,8} REBCO superconducting films with BaZrO₃ (BZO) nanocolumns have long been shown to be very effective for raising the bulk vortex pinning force density $F_p (= J_c \times B)$ at high temperatures.⁹⁻¹¹ Recently, their effectiveness has been observed at low temperatures

^aElectronic mail: axu3@central.uh.edu



too, where it appears that the large strain induced by lattice mismatch between BZO and the REBCO matrix induces a high density of point defects that pin strongly below 20–30 K, doubling F_p at 4.2 K by 7.5 mol. % Zr-doping.^{12–14} However, BZO nanorods are often detrimental to the critical temperature T_c , and any such T_c loss seriously impedes high temperature applications and blurs pinning mechanism study.^{11,15–17} Recently, by modifying the metal-organic chemical vapor deposition (MOCVD) growth process, we successfully incorporated a high density of BZO nanorods into REBCO thin films grown on standard commercial ion-beam assisted deposited (IBAD) templates without any T_c loss, a high $T_c \sim 91$ K persisting up to 20 mol. % Zr-doping.¹⁸

In our previous studies on the 7.5 mol. % Zr-doped MOCVD thin film, we observed that H_{irr} was enhanced from 8.8 to 10.2 T at 77 K, and F_p was doubled from 0.45 to 0.9 TN/m³ at 4.2 K.¹² We ascribed this excellent performance to the strong correlated pinning at high temperatures and to a high density of weak point pins at low temperatures, assigning both to the c -axis self-assembled BZO nanorods. Here, we report further enhancements at both high and low temperatures with a 15 mol. % Zr-doped MOCVD REBCO thin film. The principal goal of this work is to investigate the pinning properties of higher BZO nanorod concentrations in REBCO thin films when introduced without any T_c loss in order to assess the feasibility of further enhancing J_c and reducing the J_c anisotropy. In fact, we observed an extraordinary 45% increase in $H_{irr}(77\text{ K})$ to ~ 14.8 T, and an almost doubled and very high $F_p(4\text{ K}) \sim 1.7$ TN/m³ plateau extending from 8 T up to at least 31.2 T, values far beyond those shown by any other superconducting materials.^{19–23}

The $\sim 0.9\ \mu\text{m}$ thick (Gd, Y)BaCuO film was grown on a standard buffered IBAD Hastelloy substrate by metal-organic chemical vapor deposition.²⁴ A $\sim 2\ \mu\text{m}$ thick silver layer was deposited on the REBCO film as protection and current contact layer. Such process and structure have been scaled up to produce kilometer-long superconducting coated conductors.²⁴ To introduce c -axis aligned BZO nanorods, 15 mol. % Zr tetramethyl heptanedionate (thd) was added into the standard precursor solution so as to yield a (Gd_{0.6}Y_{0.6})Ba₂Cu_{2.3}O_x film with BZO. The 4.2 K and high field four-probe critical current measurements were performed on a $\sim 1 \times 10$ mm bridge in a 52 mm warm bore 31 T Bitter magnet fitted with a 38 mm bore liquid He cryostat at the National High Magnetic Field Laboratory (NHMFL), while the 77 K measurements were carried out on a laser-cut $\sim 50 \times 500\ \mu\text{m}$ link in a 16 T Physical Property Measurement System (PPMS). The 30 K J_c measurement was conducted on a $\sim 1 \times 10$ mm bridge in a 9 T cryocooler-driven superconducting magnet with a variable temperature insert (VTI). For the angular dependent $J_c(\theta)$ measurements, the sample was always rotated with respect to the external magnetic field around the axis parallel to the current direction in a maximum Lorentz force configuration, defining $\theta = 0$ as the applied magnetic field perpendicular to the tape plane. The critical temperature T_c is defined as the temperature where resistance $R \approx 0$, and the irreversibility field H_{irr} was determined from the field-dependent J_c with the criterion $J_c \approx 100\ \text{A/cm}^2$. Transmission electron microscopy (TEM) and atomic resolution high angle annular dark field (HAADF) scanning TEM (STEM) imaging were carried out in a JEOL ARM200cF.

Figure 1 presents representative cross-sectional and planar TEM images. Interestingly, as shown in the cross-sectional TEM [Fig. 1(a)], we observed a double-layer microstructure in which the lower half of the REBCO matrix has dense thin c -axis aligned BZO nanorods whereas the top half has a fatter and sparser BZO distribution. Figure 1(a) also shows the ~ 200 nm thick BZO nanorod free zone near the interface with the buffers, which is commonly seen in MOCVD BZO-added REBCO films. Figure 1(b) and the HAADF image in (c) show that the average diameter of BZO nanorods in the upper layer is ~ 9 nm, close to the vortex diameter $2\xi \sim 8$ nm at 77 K, suggesting why BZO nanorods are such strong pinning centers at this temperature. The corresponding matching field $B_\phi = \Phi_0/a^2$ is ~ 3.2 T, where $\Phi_0 \approx 2.07 \times 10^{-15}$ Wb is the flux quantum, and $a \approx 25$ nm is the average spacing between these BZO nanorods. The TEM image of the lower part of the film shows the BZO diameter to be ~ 6 nm and the BZO spacing to be ~ 17 nm with the corresponding B_ϕ of ~ 6.9 T. We also observed ab -plane aligned defects throughout the entire thickness, generally RE₂O₃ precipitates and stacking faults, which are also effective pins, especially along the ab -plane.

Figure 2 shows the temperature-dependent resistivity $\rho(T)$ and the superconducting transitions of both 7.5 and 15 mol. % Zr-doped films, whose room temperature resistivities (340.0 and 382.3 $\mu\Omega\text{ cm}$, respectively) are both higher than $\sim 300\ \mu\Omega\text{ cm}$ found for nominally pure REBCO

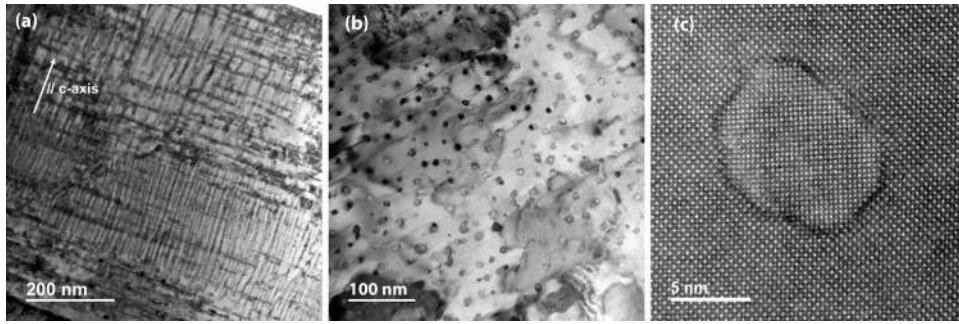


FIG. 1. (a) Cross-sectional and (b) planar TEM images of 15% Zr-doped (Gd, Y)BaCuO thin film. Interestingly, this high performance thin film exhibits the double-layer microstructure along the thickness: fat and sparse BZO nanorods at the top part, and dense thin BZO nanorods at the bottom part. The planar TEM image in (b) was taken in the top layer, the averaging spacing of BZO nanorods is ~ 25 nm. The average diameter is ~ 9 nm as seen in (c) which shows the typical cross section of a BZO nanorod. At the bottom part, the BZO spacing is ~ 17 nm, and the diameter is ~ 6 nm.

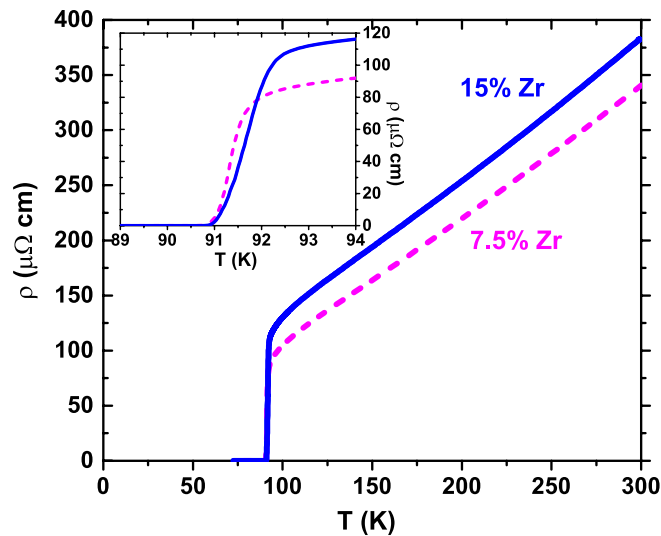


FIG. 2. Temperature-dependent resistivity $\rho(T)$ from 300 down to 72 K (solid line). Also included is $\rho(T)$ for 7.5% Zr thin film (dashed line). The inset focuses on T_c transitions. Due to the insulating nature of BZO nanorods, the 15% Zr thin film shows higher resistivity above T_c . The high T_c , ~ 91 K and sharp T_c transition are distinct from T_c loss commonly observed in BZO-doped REBCO thin films made by Pulsed Laser Deposition (PLD).

thin films, indicating that BZO is effectively incorporated inside the REBCO matrix. It is desirable to enhance pinning performance over a wide range of temperatures. In this respect, it is striking that the 15% Zr-doped thin film shows almost the same $T_c \sim 91$ K as pure and 7.5% Zr films, moreover with a sharp superconducting transition width of only ~ 1.5 K. This finding suggests a high crystalline quality of this 15% Zr-doped REBCO film, which is also supported by 2D X-ray diffraction analysis using a general area-detector diffractometer system (GADDS).¹⁸

Figure 3 displays $J_c(H)$ at 77 K for H parallel to the c -axis, and the corresponding pinning force density. In comparison with the earlier-studied 7.5% Zr-doped films, 15% Zr-doping results in much less field sensitivity of $J_c(H||c)$. Actually, J_c is lower at low magnetic fields, for example, 2.1 MA/cm² at self-field, but significantly enhanced at higher fields. With respect to J_c at self-field, the retained J_c at 3 T is $\sim 19.5\%$, and $\sim 13.4\%$ at 5 T, values much higher than the values of 10.9% at 3 T and 3.4% at 5 T measured in the 7.5% Zr-doped film. J_c remains above 0.1 MA/cm², a threshold value for applications,⁴ up to 8 T. Meanwhile, J_c of the 15% Zr-doped thin film exceeds that of Au-ion irradiated YBCO films at field above 2 T,²⁵ and the recently reported J_c of proton-irradiated metal organic deposited (MOD) thin films above 6.5 T.²⁶ Another impressive feature shown by this

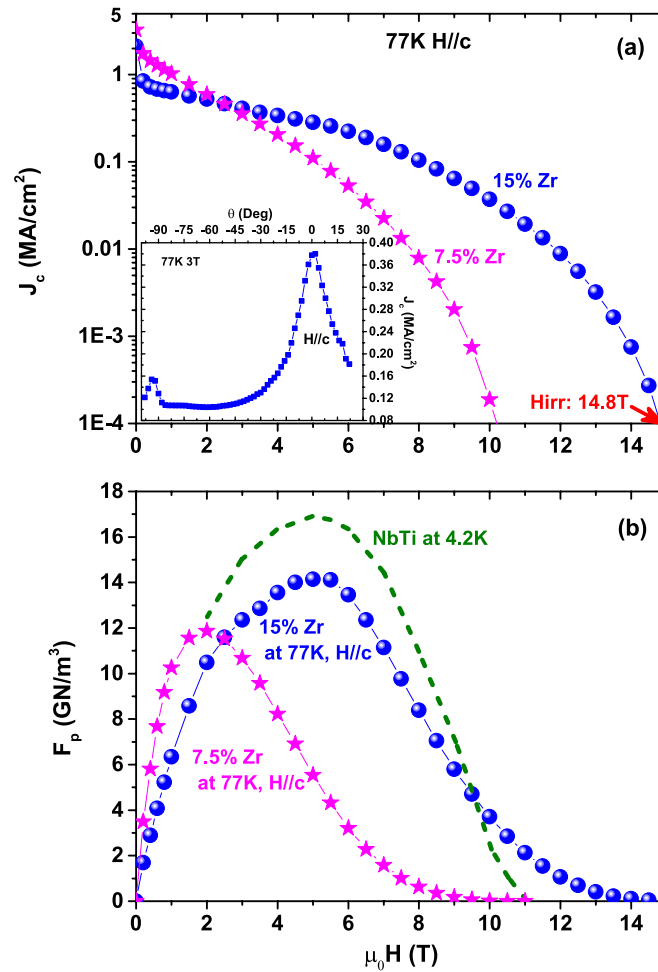


FIG. 3. (a) $J_c(H//c)$ and (b) the corresponding $F_p(H//c)$ at 77 K and H up to 15 T for both 7.5 and 15 mol. % Zr-doped films. The dotted line plots $F_p(H)$ at 4.2 K for optimized Nb-Ti wire.²¹ Ultra strong pinning of BZO nanorods is evidenced by high J_c above 0.1 MA/cm² up to 8 T. Correspondingly, $F_{p,max} \sim 14$ GN/m³ is reached at 5 T, which is comparable to the value of ~ 17 GN/m³ shown by Nb-Ti at 4.2 K. $H_{irr} \sim 14.8$ T is even higher than that of NbTi at 4.2 K. The inset shows $J_c(\theta)$ at 77 K and 3 T. The huge J_c c -axis peak manifests the strong c -axis correlated pinning provided by BZO nanorods.

sample is its extremely high $H_{irr}(77\text{ K}) \approx 14.8$ T, about 45% higher than that of the 7.5% Zr-doped film, and much higher than ~ 9 T shown by nominally pure films.

The maximum pinning force density $F_{p,max}$ reaches 14 GN/m³ at 5 T, about 18% higher than that of the 7.5% film (11.9 GN/m³), whose maximum occurred only at 2 T. Also included in Fig. 3(b) is $F_p(H)$ for optimized Nb-48 wt. %Ti wires, in which α -Ti precipitates yield significant pinning enhancement.²¹ $F_p(H//c)$ for the 15% Zr-doped film at 77 K is comparable to that of optimized Nb-Ti at 4.2 K, which is ~ 16.9 GN/m³ at ~ 5 T. Strikingly, $H_{irr}(77\text{ K}) \sim 14.8$ T for the 15% thin film is even higher than the $H_{irr} \sim 11$ T of Nb-Ti at 4.2 K. An earlier work using BaSnO₃ and BZO has achieved $F_p(H//c) > 25$ GN/m³ but peaking at somewhat lower field and without any $H_{irr}(T)$ measurement.¹⁶

$J_c(H//c)$ at 4.2 K and H up to 31.2 T of both 7.5 and 15 mol. % Zr-doped films is shown in Figure 4(a). Similar to other REBCO MOCVD thin films, $J_c(H//c)$ of the 15 mol. % Zr-doped film follows a power function over a wide field range, in this case from 8 to 31 T. However, the power exponent α is almost 1, much higher than the ~ 0.5 observed in BZO-free samples and ~ 0.7 in 7.5% Zr-doped samples,^{12,14} as shown in the inset of Fig. 4(a). The strongly varying exponent, coupled to the fact that Zr strongly enhances $J_c(4\text{ K})$, is consistent with the presence of dense, weak pinning centers in Zr-doped films that can strongly enhance J_c at temperatures less than

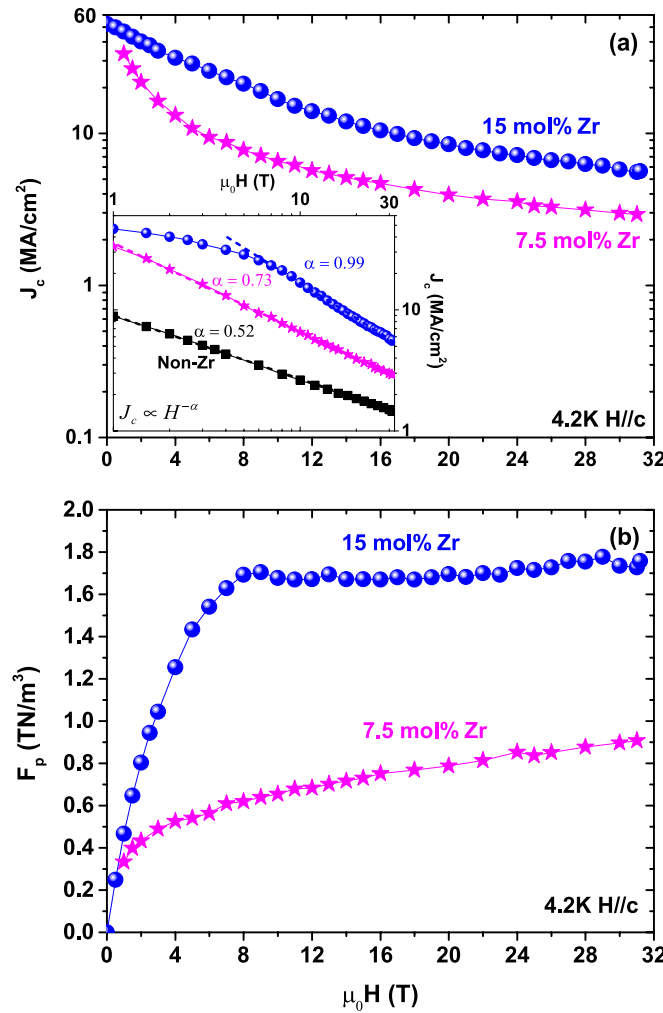


FIG. 4. (a) $J_c(H//c)$ (b) and $F_p(H//c)$ at 4.2 K under H up to 31.2 T for both 7.5 and 15 mol. % Zr-doped films. In the inset, $J_c(H//c)$ is plotted in double logarithmic scale to emphasize the power function. The exponent α for this power function is 0.99 for 15% Zr-doped thin film, much higher than ~ 0.50 shown by BZO-free film and ~ 0.73 for 7.5% Zr-doped thin film. In (b), ultra high $F_p \sim 1.7$ TN/m³, more than twice that of 7.5% Zr-doped film in the whole-studied field range, displays a plateau extending from 8 T at least up to 31.2 T.

about 30–35 K.¹² At 18 T, J_c is 9.3 MA/cm², corresponding to $I_c \approx 343$ A for standard 4 mm tape width. As Zr increases from 7.5 to 15 mol. %, J_c at 25 T is ~ 1 and ~ 3 times, respectively, improved with respect to BZO-free films. Figure 4(b) presents corresponding $F_p(H//c)$ curves. The most striking feature of the 15 mol. % Zr-doped film is its high $F_p \sim 1.7$ TN/m³ plateau extending from 8 up to at least 31 T. In the case of 7.5% Zr-doped sample, F_p increases with H up to 0.9 TN/m³ at 31.2 T but does not yet reach a maximum at this maximum accessible field.

The operating temperature for superconducting rotating machinery applications is around 30 K. $J_c(H//c)$ of the 15% Zr-doped film at 30 K is shown in Figure 5, where a power law dependent J_c is also observed above 4.5 T with $\alpha \approx 0.97$, slightly lower than $\alpha \approx 0.99$ at 4 K, and strongly in contrast to $\alpha \approx 0.6$ – 0.7 observed in REBCO thin films without BZO nanorods.^{26–29} As at 4 K, these data indicate additional weak pinning in our 15% thin film. The higher value of α is a signature that the pinning is sufficiently fine in scale, probably strain-induced point defect pinning, that it can add to the total pinning force and also be easily depinned by the strong Lorentz forces.

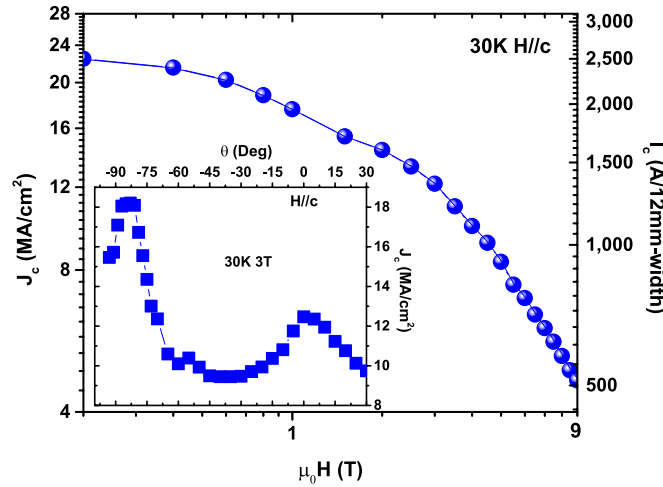


FIG. 5. $J_c(H//c)$ at 30 K in double logarithmic scale. J_c follows power-law dependence at field above ~ 4.5 T with $\alpha \approx 0.97$. The inset shows $J_c(\theta)$ at 30 K and 3 T. In contrast to 77 K, $J_c(\theta)$ renders to Ginzburg-Landau (GL)-like behavior while the c -axis peak is diminished.

J_c reaches 12.2 MA/cm² at 3 T and 7.0 MA/cm² at 6 T, and the corresponding I_c values for 12 mm wide tape are 1.4 kA at 3 T and 0.8 kA at 6 T.

Given the more than 300% J_c improvement at 4 K, 200% enhanced J_c at 30 K, and very high H_{irr} approaching 15 T at 77 K, we conclude that 15 mol. % Zr-doping is a very attractive route to high performance REBCO coated conductors with outstanding properties over the whole range of temperatures from 4 K up to 77 K under fields up to at least 31 T. The TEM images confirm the presence of self-assembled c -axis BZO nanorods. The huge J_c c -axis peak at 77 K and 3 T, as shown in the inset of Fig. 2, reveals the strong correlated pinning from the BZO nanorods, while the much higher exponent for power law dependent J_c , and the diminished J_c c -axis peak at 30 K and 3 T, as shown in the inset of Fig. 5, discloses the strong additional role of weak uncorrelated pinning stemming from strain induced by these nanorods.

The highly enhanced H_{irr} at 77 K surpasses any reported value so far for REBCO thin films regardless of the growth process.^{19,30,31} Such a high value is close and slightly higher than the H_{irr} limit ≈ 14 T proposed by Figueras *et al.* from the point of thermodynamic fluctuations of the order parameter.³² We ascribe this ultra-high H_{irr} to the synergetic effects of being able to introduce a high density of BZO nanorods without losing the starting T_c of ≈ 91 K. We should note that Muraldihar *et al.* observed a similar $H_{irr}(H//c)$ on a melt-processed (Nd_{0.33}Eu_{0.38}Gd_{0.28})Ba₂Cu₃O_y at 77 K. However, this bulk had a much higher $T_c \sim 95$ K. Similarly to us, they ascribed the strongly improved H_{irr} to dense pinning centers, in their case nanoscale lamellae of rare earth rich clusters.³³ It seems clear that there are multiple routes to obtaining good pinning properties in REBCO. What is novel in this paper is that we are able to use an industry-standard process, MOCVD on IBAD, to generate a very high J_c over an exceptionally broad range of H, T space with exceptional properties both at 4 K and at 77 K.

At present stage, we do not yet have a measure of the point pins. Llordés *et al.* proposed that the core pinning from strain-induced Cooper pair suppression dominates J_c in MOD REBCO thin films, and this mechanism explains well the observed pinning enhancement at 77 K.³⁴ In PLD thin films, by atomic-resolution Z-contrast imaging and electron energy loss spectroscopy, Cantoni *et al.* showed that the local strain between BZO nanorods and YBCO induces oxygen deficiencies surrounding BZO nanorods, and this is related to the observed T_c reduction.³⁵ Distinct from MOD and PLD films, in our MOCVD samples, our work has shown that the point defects, acting as weak uncorrelated pinning, are effective pins only at low temperatures below ~ 30 K,¹² and no T_c reduction was observed. REBCO exhibits extremely high flexibility to pinning defects.^{8,36} Other than BZO nanorods, Harrington *et al.* reported excellent pinning performance at 77 K by the incorporation of

Ra₃TaO₇ nanorods, and high $T_c \sim 91$ K was also preserved.³⁷ Feldmann *et al.* successfully added a high density of double perovskite Ba₂YNbO₆ nanorods into PLD thin films, and substantially enhanced pinning was achieved at 65 and 77 K.³⁸ So far, the low temperature and high field pinning properties of these high performance samples have not yet been reported.

In summary, 15 mol. % added Zr in a MOCVD REBCO thin film has resulted in an increase of J_c by ~ 4 times at 4.2 K. By growing such films without any T_c depression, very strong pinning properties were demonstrated at 77 K and the maximum F_p was pushed to 5 T, making $J_c(H)$ very comparable to optimized Nb-Ti at 4.2 K. These results demonstrate the immense potential for REBCO coated conductors for use at higher temperatures, perhaps even to supersede Nb-Ti and its liquid helium requirement. The enhanced performance is ascribed to the contribution of BZO nanorods to strong pinning at all temperatures, and also to a dense but weak pinning below ~ 30 K. We anticipate that even higher performance could be achieved with higher Zr contents.

We are grateful to Jianyi Jiang, Goran Majkic, Eduard Galstyan, Michael Santos, Van Griffin, and Ying Gao for discussions and experimental help. The work at the University of Houston was partially funded by Advanced Research Projects Agency-Energy (ARPA-E) award DE-AR0000196. A portion of this work was performed at the National High Magnetic Field Laboratory, which is supported by NSF Cooperative Agreement No. DMR-1157490 and by the state of Florida.

- ¹D. C. Larbalestier, A. Gurevich, D. M. Feldmann and A. A. Polyanskii, *Nature (London)* **414**, 368 (2001).
- ²V. Selvamanickam, in *Conference on Coated Conductors for Applications (CCA 2012)*, Heidelberg, Germany, 14–16 November 2012.
- ³U. P. Trociewitz, M. Dalban-Canassy, M. Hannion, D. K. Hilton, J. Jaroszynski, P. Noyes, Y. Viouchkov, H. W. Weijers, and D. C. Larbalestier, *Appl. Phys. Lett.* **99**, 202506 (2011).
- ⁴D. C. Larbalestier, J. Jiang, U. P. Trociewitz, F. Kametani, C. Scheuerlein, M. Dalban-Canassy, M. Matras, P. Chen, N. C. Craig, P. J. Lee, and E. E. Hellstrom, *Nat. Mater.* **13**, 375 (2014).
- ⁵H. W. Weijers, U. P. Trociewitz, W. D. Markiewicz, J. Jiang, D. Myers, E. E. Hellstrom, A. Xu, J. Jaroszynski, P. Noyes, Y. Viouchkov, and D. C. Larbalestier, *IEEE Trans. Appl. Supercond.* **20**, 576 (2010).
- ⁶W. D. Markiewicz, D. C. Larbalestier, H. W. Weijers, A. J. Voran, K. W. Pickard, W. R. Sheppard, J. Jaroszynski, A. Xu, R. P. Walsh, J. Lu, A. V. Gavrilin, and P. D. Noyes, *IEEE Trans. Appl. Supercond.* **22**, 4300704 (2012).
- ⁷G. Blatter, M. V. Feigel'man, V. B. Geshkenbein, A. I. Larkin, and V. M. Vinokur, *Rev. Mod. Phys.* **66**, 1125 (1994).
- ⁸S. R. Foltyn, L. Civale, J. L. MacManus-Driscoll, Q. X. Jia, B. Maiorov, H. Wang, and M. Maley, *Nat. Mater.* **6**, 631 (2007).
- ⁹J. L. MacManus-Driscoll, S. R. Foltyn, Q. X. Jia, H. Wang, A. Serquis, L. Civale, B. Maiorov, M. E. Hawley, M. P. Maley, and D. E. Peterson, *Nat. Mater.* **3**, 439 (2004).
- ¹⁰S. Kang, A. Goyal, J. Li, A. A. Gapud, P. M. Martin, L. Heatherly, J. R. Thompson, D. K. Christen, F. A. List, M. Paranthaman, and D. F. Lee, *Science* **311**, 1911 (2006).
- ¹¹Y. Chen, V. Selvamanickam, Y. Zhang, Y. Zuev, C. Cantoni, E. Specht, M. P. Paranthaman, T. Aytug, A. Goyal, and D. Lee, *Appl. Phys. Lett.* **94**, 062513 (2009).
- ¹²A. Xu, V. Braccini, J. Jaroszynski, Y. Xin, and D. C. Larbalestier, *Phys. Rev. B* **86**, 115416 (2012).
- ¹³A. Xu, J. Jaroszynski, F. Kametani, Z. Chen, D. C. Larbalestier, Y. L. Viouchkov, Y. Chen, Y. Xie, and V. Selvamanickam, *Supercond. Sci. Technol.* **23**, 014003 (2010).
- ¹⁴V. Braccini, A. Xu, J. Jaroszynski, Y. Xin, D. C. Larbalestier, Y. Chen, G. Carota, J. Dackow, I. Kesgin, Y. Yao, A. Guevara, T. Shi, and V. Selvamanickam, *Supercond. Sci. Technol.* **24**, 035001 (2011).
- ¹⁵T. Aytug, M. Paranthaman, E. D. Specht, Y. Zhang, K. Kim, Y. L. Zuev, C. Cantoni, A. Goyal, D. K. Christen, V. A. Maroni, Y. Chen, and V. Selvamanickam, *Supercond. Sci. Technol.* **23**, 014005 (2010).
- ¹⁶P. Mele, K. Matsumoto, T. Horide, A. Ichinose, M. Mukaida, Y. Yoshida, S. Horii, and R. Kita, *Supercond. Sci. Technol.* **21**, 032002 (2008).
- ¹⁷S. H. Wee, Y. L. Zuev, C. Cantoni, and A. Goyal, *Sci. Rep.* **3**, 2310 (2013).
- ¹⁸V. Selvamanickam, Y. Chen, T. Shi, Y. Liu, N. D. Khatri, J. Liu, Y. Yao, X. Xiong, C. Lei, S. Soloveichik, E. Galstyan, and G. Majkic, *Supercond. Sci. Technol.* **26**, 035006 (2013).
- ¹⁹J. Gutiérrez, A. Llordés, J. Gázquez, M. Gibert, N. Romà, S. Ricart, A. Pomar, F. Sandiumenge, N. Mestres, T. Puig, and X. Obradors, *Nat. Mater.* **6**, 367 (2007).
- ²⁰J. D. Weiss, C. Tarantini, J. Jiang, F. Kametani, A. A. Polyanskii, D. C. Larbalestier, and E. E. Hellstrom, *Nat. Mater.* **11**, 682 (2012).
- ²¹C. Meingast and D. C. Larbalestier, *J. Appl. Phys.* **66**, 5971 (1989).
- ²²J. Jiang, H. Miao, Y. Huang, S. Hong, J. A. Parrell, C. Scheuerlein, M. D. Michiel, K. Ghosh, U. P. Trociewitz, E. E. Hellstrom, and D. C. Larbalestier, *IEEE Trans. Appl. Supercond.* **23**, 6400206 (2013).
- ²³B. J. Senkovicz, J. E. Giencke, S. Patnaik, C. B. Eom, E. E. Hellstrom, and D. C. Larbalestier, *Appl. Phys. Lett.* **86**, 202502 (2005).
- ²⁴V. Selvamanickam, Y. Chen, X. Xiong, Y. Xie, M. Martchevski, A. Rar, Y. Qiao, R. M. Schmidt, A. Knoll, K. P. Lenseth, and C. S. Weber, *IEEE Trans. Appl. Supercond.* **19**, 3225 (2009).
- ²⁵H. Matsui, H. Ogisio, H. Yamasaki, T. Kumagai, M. Sohma, I. Yamaguchi, and T. Manabe, *Appl. Phys. Lett.* **101**, 232601 (2012).

- ²⁶ Y. Jia, M. LeRoux, D. J. Miller, J. G. Wen, W. K. Kwok, U. Welp, M. W. Rupich, X. Li, S. Sathyamurthy, S. Fleshler, A. P. Malozemoff, A. Kayani, O. Ayala-Valenzuela, and L. Civale, *Appl. Phys. Lett.* **103**, 122601 (2013).
- ²⁷ C. J. van der Beek, M. Konczykowski, A. Abal'oshev, I. Abal'osheva, P. Gierlowski, S. J. Lewandowski, M. V. Indenbom, and S. Barbanera, *Phys. Rev. B* **66**, 024523 (2002).
- ²⁸ M. Miura, B. Maiorov, S. A. Baily, N. Haberkorn, J. O. Willis, K. Marken, T. Izumi, Y. Shiohara, and L. Civale, *Phys. Rev. B* **83**, 184519 (2011).
- ²⁹ A. O. Ijaduola, J. R. Thompson, R. Feenstra, D. K. Christen, A. A. Gapud, and X. Song, *Phys. Rev. B* **73**, 134502 (2006).
- ³⁰ M. Miura, S. A. Baily, B. Maiorov, L. Civale, J. O. Willis, K. Marken, T. Izumi, K. Tanabe, and Y. Shiohara, *Appl. Phys. Lett.* **96**, 072506 (2010).
- ³¹ A. Kiessling, J. Hänisch, T. Thersleff, E. Reich, M. Weigand, R. Hühne, M. Sparing, B. Holzapfel, J. H. Durrell, and L. Schultz, *Supercond. Sci. Technol.* **24**, 055018 (2011).
- ³² J. Figueras, T. Puig, X. Obradors, W. K. Kwok, L. Paulius, G. W. Crabtree, and G. Deutscher, *Nat. Phys.* **2**, 402 (2006).
- ³³ M. Muralidhar, N. Sakai, N. Chikumoto, M. Jirsa, T. Machi, M. Nishiyama, Y. Wu, and M. Murakami, *Phys. Rev. Lett.* **89**, 237001 (2002).
- ³⁴ A. Llordés, A. Palau, J. Gázquez, M. Coll, R. Vlad, A. Pomar, J. Arbiol, R. Guzmán, S. Ye, V. Rouco, F. Sandiumenge, S. Ricart, T. Puig, M. Varela, D. Chateigner, J. Vanacken, J. Gutiérrez, V. Moshchalkov, G. Deutscher, C. Magen, and X. Obradors, *Nat. Mater.* **11**, 329 (2012).
- ³⁵ C. Cantoni, Y. Gao, S. H. Wee, E. D. Specht, J. Gázquez, J. Meng, S. J. Pennycook, and A. Goyal, *ACS Nano* **5**, 4783 (2011).
- ³⁶ K. Matsumoto and P. Mele, *Supercond. Sci. Technol.* **23**, 014001 (2010).
- ³⁷ S. A. Harrington, J. H. Durrell, B. Maiorov, H. Wang, S. C. Wimbush, A. Kursumovic, J. H. Lee, and J. L. MacManus-Driscoll, *Supercond. Sci. Technol.* **22**, 022001 (2009).
- ³⁸ D. M. Feldmann, T. G. Holesinger, B. Maiorov, S. R. Foltyn, J. Y. Coulter, and I. Apodaca, *Supercond. Sci. Technol.* **23**, 095004 (2010).